![PCCP journal cover: Volume 1 | Number 1 | Jan 2013 | Pages 1–100. PCCP Physical Chemistry Chemical Physics www.rsc.org/pccp. Royal Society of Chemistry.]

Journal Name

ARTICLE

Structural and silver/vanadium ratio effects on silver vanadium phosphorous oxide solution formation kinetics: impact on battery electrochemistry

David C. Bock,[a] Kenneth J. Takeuchi,[a,b]* Amy C. Marschilok,[a,b]* and Esther S. Takeuchi[a,b,c]*

The detailed understanding of non-Faradaic parasitic reactions which diminish battery calendar life is essential to the development of effective batteries for use in long life applications. The dissolution of cathode materials including manganese, cobalt and vanadium oxides in battery systems has been identified as a battery failure mechanism, yet detailed dissolution studies including kinetic analysis are absent from the literature. The results presented here provide a framework for the quantitative and kinetic analyses of the dissolution of cathode materials which will aid the broader community in more fully understanding this battery failure mechanism. In this study, the dissolution of silver vanadium oxide, representing the primary battery powering implantable cardioverter defibrillators (ICD), is compared with the dissolution of silver vanadium phosphorous oxide ($Ag_wV_xP_yO_z$) materials which were targeted as alternatives to minimize solubility. This study contains the first kinetic analyses of silver and vanadium solution formation from $Ag_{0.48}VOPO_4 \cdot 1.9H_2O$ and $Ag_2VP_2O_8$, in a non-aqueous battery electrolyte. The kinetic results are compared with those of $Ag_2VO_2PO_4$ and $Ag_2V_4O_{11}$ to probe the relationships among crystal structure, stoichiometry, and solubility. For vanadium, significant dissolution was observed for $Ag_2V_4O_{11}$ as well as for the phosphate oxide $Ag_{0.49}VOPO_4 \cdot 1.9H_2O$, which may involve structural water or the existence of multiple vanadium oxidation states. Notably, the materials from the SVPO family with the lowest vanadium solubility are $Ag_2VO_2PO_4$ and $Ag_2VP_2O_8$. The low concentrations and solution rates coupled with their electrochemical performance make these materials interesting alternatives to $Ag_2V_4O_{11}$ for the ICD application.

Introduction

Implantable medical devices present distinctive challenges for new battery research. For example, new batteries for implantable medical devices must pass the most stringent of requirements regarding safety and reliability.[1] Further, long calendar life is an equally important characteristic since surgical replacement of the battery incurs high costs as well as potential medical issues for the patient.

In order to address safety and reliability concerns as well as battery lifetimes, a critical basic research goal is the understanding and subsequent minimization of non-Faradaic parasitic reactions that can negatively affect the longevity of implantable battery systems. An authentic example of non-Faradaic reactions within a battery is the solution formation of the battery cathode material into the electrolyte. Cathode

solubility is problematic since the loss of useable electrode material will decrease the battery capacity. In addition to a reduction in battery capacity, cathode materials in solution can interact with the anode resulting in a modification of the passivation layer on the anode surface with an increase in cell polarization and a concomitant decrease in electrochemical battery performance. Perhaps due to the subtlety and complexity of cathode solution effects on battery electrochemistry, which may occur in practice over months or years, there are relatively few studies of the kinetics of cathode solution formation for non-aqueous batteries.[2-7]

The Li/SVO battery[8-12] is a primary battery which remains the benchmark technology for use in implantable cardioverter defibrillator (ICD) devices. ICD devices apply a high watt pulse to a patient's heart to address ventricular fibrillation. The Li/SVO battery provides the high power necessary to charge the pulse delivering capacitors of the ICD and has suitably high

capacity for multiple years of use. However, solubility of the $Ag_2V_4O_{11}$ is a known major life limiting mechanism. Vanadium species dissolved into the electrolyte deposit onto the lithium anode surface, increasing the DC resistance of the cell.[13] If pulse power capability is sufficiently diminished, the battery is no longer effective and replacement is required.

In order to understand the solution formation of the $Ag_2V_4O_{11}$ cathode in non-aqueous solvents, we have chosen to investigate the silver vanadium phosphorous oxide ($Ag_wV_xP_yO_z$) family of materials, which exhibit electrochemical performance characteristics which are suitable for ICDs and other high rate applications, yet are structurally reminiscent of $Ag_2V_4O_{11}$. This strategy is based on the hypothesis that phosphate based cathode materials would reduce cathode component concentrations in the electrolyte, as the strong covalent P-O bonds from the inclusion of PO_4^{3-} polyanions stabilize the vanadium oxide framework.[14, 15] In support of this idea are previous studies which show that the phosphate based cathode material $LiFePO_4$ provides higher stability in electrolyte relative to oxide based materials.[16, 17]

Our study of the solution formation of silver and vanadium from the silver vanadium phosphorous oxide (SVPO) material $Ag_2VO_2PO_4$ and the benchmark $Ag_2V_4O_{11}$ material was the first of several related reports from our laboratories. The equilibrium vanadium concentration in a battery electrolyte (1M $LiBF_4$ in propylene carbonate:dimethoxyethane) was approximately 5 times lower for $Ag_2VO_2PO_4$ compared with $Ag_2V_4O_{11}$, providing evidence that use of the SVPO material in ICD batteries could be effective in reducing solubility and thus potentially increasing service life.[18] In our subsequent report the appearance of silver in addition to vanadium in the electrolyte was discussed. Notably, the levels of silver and vanadium dissolved in the electrolyte did not reflect the stoichiometry of the solids, indicating that the mechanism(s) by which silver and vanadium appear in solution are more complex than simple stoichiometric dissolution.[19] Further, it was also found that changing the particle size of the $Ag_2VO_2PO_4$ by synthesizing it under a different method had an effect on the observed solution formation kinetics, but no significant impact on the long term solubility of vanadium. This study highlighted the criticality of crystal structure relative to BET surface area in terms of dictating vanadium solubility.

Our studies of other members of the material class of silver vanadium phosphorous oxides yielded electrochemistries promising for implementation in high power applications, including ICD batteries. The discharge profile of $Ag_{0.48}VOPO_4·1.9H_2O$ remains above 3.0 V for a large portion of the discharge, and there are multiple plateaus which are advantageous for end of service notification, with good pulse discharge capability.[20, 21] In terms of composition, $Ag_{0.48}VOPO_4·1.9H_2O$ is distinct from $Ag_2VO_2PO_4$ in that water molecules are incorporated into its structure. Also significant is that vanadium exists in two oxidation states, V(IV) and V(V).

$Ag_2VP_2O_8$ is a third member of the SVPO family we investigated as a primary battery cathode material.[22] As with $Ag_2VO_2PO_4$, $Ag_2VP_2O_8$ displays in-situ formation of silver metal nanoparticles when it is initially reduced, improving the cathode conductivity. Continued discharge results in fracture of the particles, however, which reduces the conductivity significantly. $Ag_2VP_2O_8$ is unique from the other silver vanadium phosphorous oxides in that it is a diphosphate material. The presence of the diphosphate anion may play a role in influencing solution formation from the material and will be considered when analyzing the results.

In order to better probe the relationships between material structure and solution formation, this paper presents the first solution formation analysis of two other members of the silver vanadium phosphorous oxide family, $Ag_{0.48}VOPO_4·1.9H_2O$, and $Ag_2VP_2O_8$, with $Ag_2VO_2PO_4$ and $Ag_2V_4O_{11}$ materials used as comparative benchmarks. Elucidation of the non-Faradaic parasitic reactions of the materials in the battery environment and determination of their relationship to calendar life is a particularly important consideration for implantable medical batteries, especially for devices powering essential life functions such as cardiac rhythm devices. By investigating a family of compositionally related yet structurally different materials, insight into the deterministic structure factors influencing long term stability of energy storage materials will be gained. These results will identify which members of the SVPO material family show the most promise for reducing cathode solution concentrations in battery electrolyte while also providing appropriate electrochemistry as cathode materials.

Notably, there are several cathode systems which show solubility as a function of state of discharge which would benefit significantly from this type of analysis. Cells using $LiMn_2O_4$ cathodes can exhibit long-term degradation of key performance metrics due to Mn dissolution.[3, 4, 6, 23-26] One of the observed physical effects has been deposition of Mn on the anode in the cell.[23, 26-28] These deposited species increase the impedance of the electrode and cause self-discharge of the lithiated carbon, resulting in capacity fade.[23] LiV_3O_8 is another cathode material which dissolves into non-aqueous electrolytes.[7, 29-31] The dissolution is observed from the discharged material, and is thought to contribute to capacity fade upon cycling. Similar to $LiMn_2O_4$, deposition of the dissolved species on the anode has been observed.[30] Cathode dissolution from $LiCoO_2$ and subsequent deposition of Co on the negative electrode has also been reported.[2, 32-34] Analysis of $Li/LiCoO_2$ cells cycled above 4.2 V indicated a direct correlation between capacity fade and cobalt deposition on the anode.[2] Based on these reports, the dissolution of cathode materials into non-aqueous electrolyte is a widespread issue for many battery materials in addition to the specific examples described in this study. The results presented here provide a framework for both the quantitative and kinetic analysis of the dissolution of cathode materials which will aid the broader community in more fully understanding this battery failure mechanism.

Experimental Section

Materials Synthesis and Characterization

Silver vanadium oxide ($Ag_2V_4O_{11}$) was prepared via a previously reported solid state reaction method.[10] $Ag_2VO_2PO_4$ was synthesized by a hydrothermal reaction method reported in the literature.[35] Adaptation of a previously reported hydrothermal method was also used to prepare $Ag_{0.49}VOPO_4·1.9H_2O$.[36] $Ag_2VP_2O_8$ was prepared via a solid state reaction as reported.[37]

Differential scanning calorimetry (DSC) analysis was performed using a TA instruments Q20 and thermogravimetric analysis (TGA) was performed using a TA instruments SDT Q600. Powder X-ray diffraction (XRD) measurements were recorded with a Rigaku Smart Lab X-ray diffractometer with Cu Kα radiation and Bragg-Brentano focusing geometry. Elemental analysis was done using inductively coupled plasma optical emission spectroscopy (ICP-OES) with a Thermo Scientific iCAP 6000 series spectrometer. Surface area determination was done with a using the multipoint BET (Brunauer, Emmett, and Teller) method.

Dissolution Analysis

Each compound was immersed in electrolyte solution under inert atmosphere conditions at ambient temperature. The electrolyte consisted of 1M $LiBF_4$ dissolved in propylene carbonate where water content by Karl Fisher titration was less than 40 ppm. At specified intervals an aliquot of electrolyte was removed from each parent sample and analyzed via ICP-OES to determine the dissolved concentration of silver and vanadium ions. In order to account for the small volumes of electrolyte removed from the parent samples at each measurement point, a correction calculation, described previously,[21] was applied to the data.

Results and Discussion

Materials Characterization

The low silver ratio silver vanadium phosphorous oxide, $Ag_{0.49}VOPO_4 \cdot 1.9H_2O$, was characterized using a combination of techniques, including inductively coupled plasma optical emission spectroscopy (ICP-OES), thermogravimetric analysis (TGA) and XRD. The silver to vanadium ratio was determined to be 0.49 by ICP-OES, which is a slightly higher silver content than the value of 0.43 reported in the original literature[36] and consistent with the Ag/V ratio of 0.48 published in a more recent paper.[20] Thermogravimetric analysis was used to determine the water content of the material at 1.9 water molecules per formula unit. The formula of the material was then assigned as $Ag_{0.49}VPO_4 \cdot 1.9H_2O$. Surface area was 1.0 ± 0.1 m^2/g.

The experimentally recorded pattern of the synthesized $Ag_{0.49}VOPO_4 \cdot 1.9H_2O$ material compared well with the reference pattern for $Ag_{0.43}VOPO_4 \cdot 2H_2O$ (PDF#00-052-1416). Structurally, the material crystallizes in a layered structure with a V-O-P-O framework.[36] (Figure 1i) Silver ions and water molecules are located between the layers. Ag is in a distorted octahedral environment, with four of the oxygens being associated with water molecules and the remaining two oxygens part of the V-O-P-O layer.
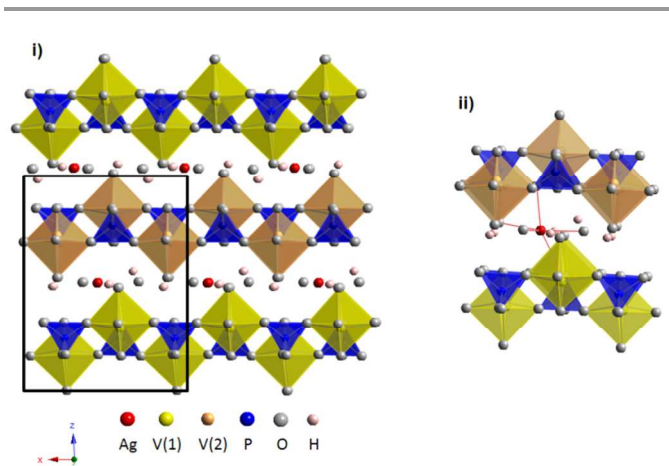

Figure 1i. Crystal structure of $Ag_{0.43}VOPO_4 \cdot 2H_2O$ viewed along the b axis, emphasizing the V-O-P-O layer framework. **ii.** Proposed coordination environment of Ag^+ ions at the edge of the structure.

The second silver vanadium phosphorous oxide was characterized and confirmed as $Ag_2VP_2O_8$. ICP-OES showed the Ag/V ratio of 2:1 and the V/P ratio of 1/2. BET surface area of the synthesized material was 0.7 ± 0.1 m^2/g. The XRD of the synthesized material matched the reference pattern[37] (PDF #01-088-0436). The diphosphate structure of $Ag_2VP_2O_8$ (Figure 2i) is characterized by layers stacking along the [010] direction, with those layers consisting of interconnecting $[V_2P_2O_8]_\infty$ chains running parallel to the [100] direction.[37] Vanadium resides in a VO_6 octahedron having five corners shared with five P^{5+} tetrahedrons and the 6th oxygen unshared with neighboring polyhedra.[22] The vanadium in the octahedron is located nearer to the unshared oxygen, giving long and short bond lengths.[22] Monovalent Ag^+ cations are located in two independent sites, with Ag(1) and Ag(2) located in tunnels.
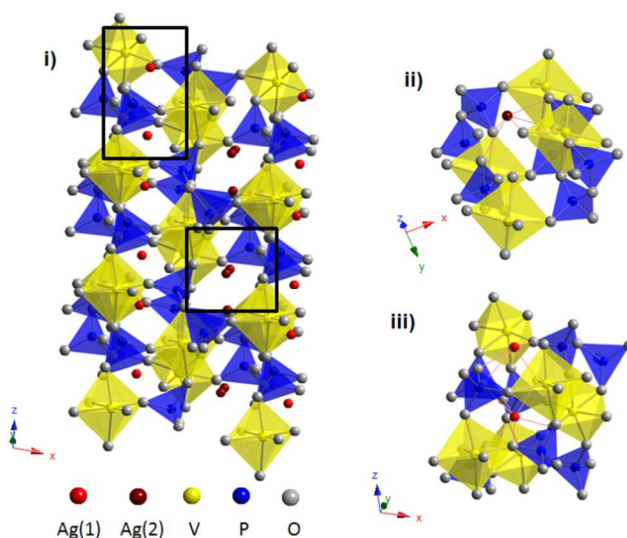

Figure 2i. Crystal structure of $Ag_2VP_2O_8$ viewed along the b axis. Proposed incomplete coordination environments of **ii.** $Ag(2)^+$ ions and **iii.** $Ag(1)^+$ ions located at the edge of tunnels above the plane of VO_6 and PO_4 polyhedra.

Vanadium Dissolution

Average vanadium ion concentrations as a function of time for $Ag_{0.49}VOPO_4 \cdot 1.9H_2O$ and $Ag_2VP_2O_8$ are plotted in Figure 3. The experiment was repeated with 11 replicate samples for $Ag_{0.49}VOPO_4 \cdot 1.9H_2O$ and 12 replicate samples for $Ag_2VP_2O_8$ and the error bars shown represent one standard deviation from the mean values. Lower concentrations of vanadium were observed with the $Ag_2VP_2O_8$ sample compared to the $Ag_{0.49}VOPO_4 \cdot 1.9H_2O$ material. In order to quantify the solution formation results, the vanadium concentration-time data was fit using the Noyes-Whitney equation for the solution formation of solid particles in liquid media.[38] The integrated form of this equation is

$$C = C_s[1 - \exp(-kt)] \qquad (1)$$

where C is the concentration of the solid in solution at time t, C_s is the equilibrium solubility at the particle surface, and k is a first order rate constant. This equation represents a physical mechanism whereby solvated molecules are transported from the solid/liquid interface through a thin boundary layer to the bulk solution.[39] The concentration gradient between the solid/liquid interface and the bulk solution drives the diffusion process.
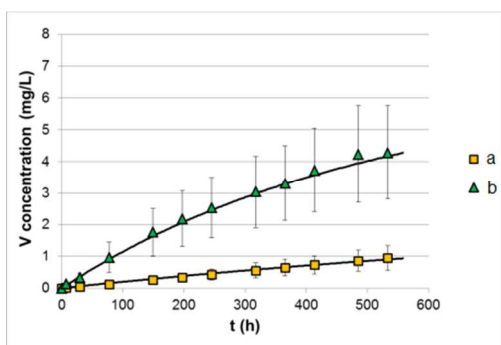

Figure 3. Overlays of Noyes-Whitney fits to average vanadium concentration vs. time data for a) $Ag_2VP_2O_8$ and b) $Ag_{0.49}VOPO_4 \cdot 1.9H_2O$.

Non-linear regression analysis was used to fit the integrated Noyes-Whitney equation to the experimental vanadium solution formation data and evaluate the parameters C_s and k. The average and standard deviation of these parameters as well as the coefficient of determination values for the fits for the individual trials are compiled in Table 1. The best fits of the equation to the averaged data are shown as solid lines in Figure 3 for the two materials. $Ag_{0.49}VOPO_4 \cdot 1.9H_2O$ was determined to have an equilibrium solubility C_s of 7 ± 2 mg/L. In contrast, $Ag_2VP_2O_8$ had a lower equilibrium solubility of 3 ± 1 mg/L. The rate constant for the solution formation was also lower for $Ag_2VP_2O_8$, compared with $Ag_{0.49}VOPO_4 \cdot 1.9H_2O$. The lower rate constant for $Ag_2VP_2O_8$ is consistent with the observation that after three weeks, the data do not appear to come to an equilibrium concentration. The high coefficients of determination for the fit indicate that the solution formation data through three weeks is consistent with diffusion layer mechanism described by equation 1.

Material	C_s (mg/L)	k (s^{-1})	R^2
$Ag_{0.49}VOPO_4 \cdot 1.9H_2O$	7 ± 2	$5.7E\text{-}7 \pm 1.8E\text{-}7$	0.99 ± 0.01
$Ag_2VP_2O_8$	3 ± 1	$2.3E\text{-}7 \pm 6.5E\text{-}8$	0.97 ± 0.03

Table 1. Average Noyes-Whitney fitting parameters for vanadium solution formation from $Ag_2VP_2O_8$ (n=12) and $Ag_{0.49}VOPO_4 \cdot 1.9H_2O$ (n=11).

Silver Dissolution

The solubility of silver from the materials was also investigated. Figure 4 plots the average fraction of silver dissolved from the various materials versus time for $Ag_{0.49}VOPO_4 \cdot 1.9H_2O$ and $Ag_2VP_2O_8$. Data points represent the mean value of 11 or 12 individual samples of each material, with error bars signifying one standard deviation. The general curve of the solution formation profiles of silver at higher electrolyte salt concentrations can be described as having a steeper initial slope for the initial 0-24 hours of exposure to electrolyte, with the concentration then rising at a lower rate. The silver concentration-time data cannot be adequately modeled by the Noyes-Whitney equation describing solid solution formation, thus, the Weibull distribution function[40], first used by Langenbucher to describe solution formation data[41], was used for fitting the experimental results. The general form of the Weibull distribution for describing solution formation data is:

$$m = 1 - \exp(-\alpha t^\beta) \qquad (2)$$

where m is the accumulated fraction of dissolved material at time t, α is a time scaling constant, and β is a constant which defines the shape of the curve. In cases where the solution formation curve has an exponential shape, $\beta = 1$. If the curve is S-shaped, $\beta > 1$, and if the curve has a higher initial slope followed by consistency with the exponential, $\beta < 1$.[42, 43]
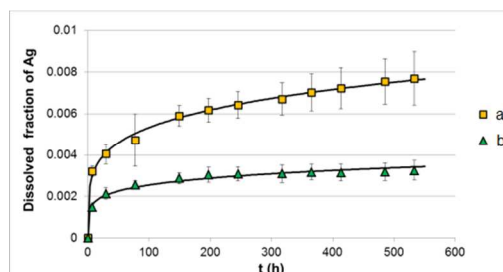

Figure 4. Overlays of Weibull fits to average dissolved fraction of Ag vs. time data a) $Ag_2VP_2O_8$ and b) $Ag_{0.49}VOPO_4 \cdot 1.9H_2O$.

The Weibull function has been used previously to empirically describe the solution formation of pharmaceutical drugs.[44-54] The Weibull function can be viewed as representing a first order process with a time-dependent rate coefficient.[42] The Weibull function has also been previously used to describe solution formation of Ag from $Ag_2VO_2PO_4$ and $Ag_2V_4O_{11}$.[21]

The silver concentration vs. time data for $Ag_{0.49}VOPO_4 \cdot 1.9H_2O$ and $Ag_2VP_2O_8$ was converted to accumulated fraction of dissolved material vs. time, and the Weibull distribution was then fit to the data using non-linear regression analysis. The average and standard deviation of the fitting parameters for the 11 and 12 individual trials of each material are compiled in Table 2. The best fits of the function to the experimental results are illustrated in Figure 4. The coefficients of determination indicate that the Weibull distribution was an acceptable function for modeling the solution formation of silver from the two materials.

Material	α	β	R^2
$Ag_{0.49}VOPO_4 \cdot 1.9H_2O$	2.8E-4 ± 1.3E-4	0.18 ± 0.046	0.97 ± 0.02
$Ag_2VP_2O_8$	4.2E-4 ± 2.8E-4	0.21 ± 0.054	0.99 ± 0.05

Table 2. Average Weibull function fitting parameters for silver solution formation from $Ag_2VP_2O_8$ (n=12) and $Ag_{0.49}VOPO_4 \cdot 1.9H_2O$ (n=11).

Comparison of Dissolution Results with $Ag_2VO_2PO_4$ and $Ag_2V_4O_{11}$

The solubility of $Ag_2VO_2PO_4$ and $Ag_2V_4O_{11}$, has recently been described.[18, 19] The mean vanadium concentration vs. time data for $Ag_2VO_2PO_4$ and $Ag_2V_4O_{11}$ is overlaid with the data for $Ag_{0.49}VPO_4 \cdot 1.9H_2O$ and $Ag_2VOP_2O_8$, Figure 5. The best fit for the Noyes-Whitney function through the mean data for each material is represented as a black line. A comparison of the mean levels of the vanadium dissolved for each material after 22 days is plotted in Figure 6A. From the two charts, it is clear that the oxide material $Ag_2V_4O_{11}$ dissolved a higher level of vanadium than any of the silver vanadium phosphorous oxide compounds, with a mean concentration of 7.6 mg/L at 21 days. Among the SVPO materials, $Ag_{0.49}VOPO_4 \cdot 1.9H_2O$ had the highest level of vanadium solution formation, at 4.3 mg/L. Vanadium solution formation was lower for $Ag_2VO_2PO_4$ and $Ag_2VP_2O_8$. However, in comparing these two materials, the Noyes Whitney fits to the data suggest that $Ag_2VP_2O_8$ may dissolve more slowly than $Ag_2VO_2PO_4$ but have a higher equilibrium concentration.

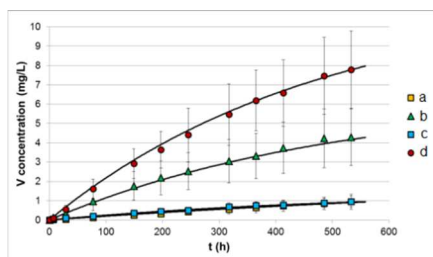**Figure 5.** Overlays of Noyes-Whitney fits to average vanadium concentration vs. time data for a) $Ag_2VP_2O_8$ b) $Ag_{0.49}VOPO_4 \cdot 1.9H_2O$ c) $Ag_2VO_2PO_4$ and d) $Ag_2V_4O_{11}$
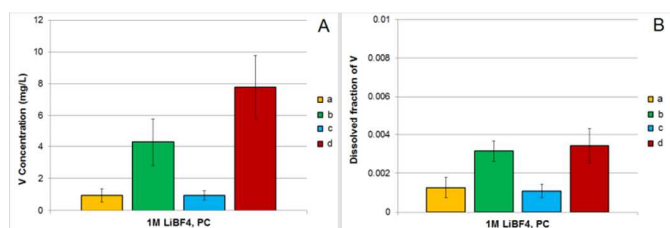

Figure 6A. Average concentration of dissolved vanadium and **B.** average dissolved fraction of vanadium at 22 days for a) $Ag_2VP_2O_8$ b) $Ag_{0.49}VOPO_4 \cdot 1.9H_2O$ c) $Ag_2VO_2PO_4$ and d) $Ag_2V_4O_{11}$

Silver solution formation from the four target materials was also compared. Figure 7A shows the mean silver concentration versus time data, while Figure 7B plots the accumulated fraction of dissolved material vs. time, with the best fit for the Weibull function through the mean data for each material represented as a black line. Figure 8A shows bar charts comparing the mean levels of silver dissolved for each material

after 22 days. $Ag_2VP_2O_8$ dissolved the most Ag after 22 days, with an average concentration of approximately 23 mg/L.

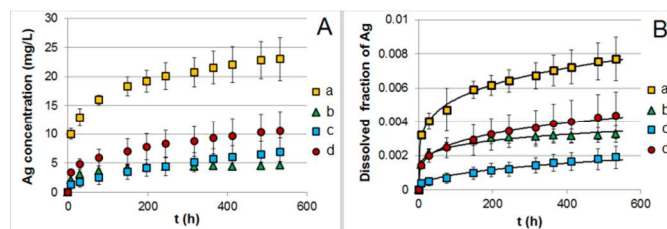**Figure 7A.** Average silver concentration vs. time data and B. Weibull fits to average dissolved fraction of Ag vs. time for a) $Ag_2VP_2O_8$ b) $Ag_{0.49}VOPO_4 \cdot 1.9H_2O$ c) $Ag_2VO_2PO_4$ and d) $Ag_2V_4O_{11}$.
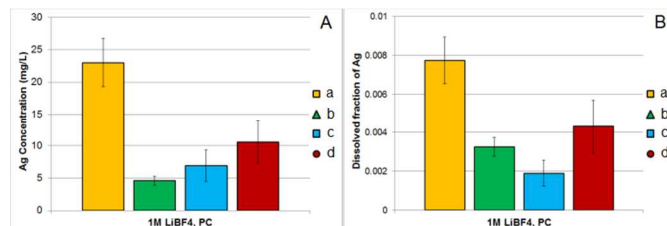

Figure 8A. Average concentration of dissolved silver and **B.** average dissolved fraction of silver at 22 days for a) $Ag_2VP_2O_8$ b) $Ag_{0.49}VOPO_4 \cdot 1.9H_2O$ c) $Ag_2VO_2PO_4$ and d) $Ag_2V_4O_{11}$.

Normalized solution formation values

The solution formation of silver and vanadium from the various target materials can also be normalized to account for the differences in stoichiometry. This was accomplished by dividing the moles of silver or vanadium dissolved by the number of moles of silver or vanadium in the target material exposed to electrolyte. Normalized vanadium and silver solution formation data are exhibited in Figures 7B and 9, respectively. From the normalized data, the rank order of moles silver dissolved per mole exposed to electrolyte, from highest to lowest, was $Ag_2VP_2O_8$, $Ag_2V_4O_{11}$, $Ag_{0.49}VOPO_4 \cdot 1.9H_2O$, and $Ag_2VO_2PO_4$. The normalized level of Ag solution formation from $Ag_2VP_2O_8$ is approximately double that of the other two phosphate based materials. The normalized vanadium solution formation data indicates that $Ag_{0.49}VOPO_4 \cdot 1.9H_2O$ and $Ag_2V_4O_{11}$ had the highest levels of moles vanadium dissolved per mole vanadium exposed to electrolyte. The average normalized vanadium solution formation values from these materials was approximately three times that of the other two phosphate based materials, $Ag_2VP_2O_8$ and $Ag_{0.49}VOPO_4 \cdot 1.9H_2O$.

To test the hypothesis that Ag^+ solution formation proceeds by an ion exchange mechanism with Li^+ ions in the electrolyte salt, initial solution formation of Ag and V were tested in both propylene carbonate only and propylene carbonate with 1M $LiBF_4$. In propylene carbonate solvent with no electrolyte salt added, only trace levels (<0.1 mg/L) of Ag dissolved into the electrolyte. In contrast, a high rate of Ag solution formation was observed after only 3 hours of exposure to the PC 1M $LiBF_4$, with concentrations after 3 hours of 1.1, 2.7, 3.4 and 5.8 mg/L for $Ag_2VO_2PO_4$, $Ag_2VP_2O_8$, $Ag_{0.49}VOPO_4 \cdot 1.9H_2O$, $Ag_2V_4O_{11}$, and $Ag_2VP_2O_8$, respectively. This data supports the hypothesis that Li^+ ion exchange with Ag^+ plays a significant role in terms of the amount of silver detected in solution. The

vanadium levels dissolved were low and similar in solutions with and without electrolyte salt, <0.3 mg/L in all cases.
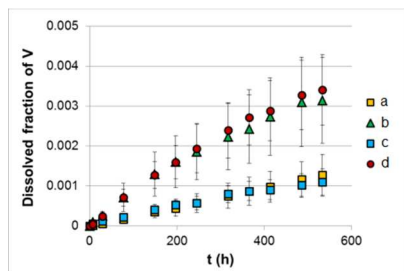

Figure 9. Average dissolved fraction of V vs. time for a) $Ag_2VP_2O_8$ b) $Ag_{0.49}VOPO_4 \cdot 1.9H_2O$ c) $Ag_2VO_2PO_4$ and d) $Ag_2V_4O_{11}$.

Discussion

The levels of vanadium and silver dissolved from the cathode materials are less than 0.1% of the total amount of material exposed to electrolyte, as seen from the solution formation data. Therefore, all of the target materials are relatively insoluble in the electrolyte tested. It is reasonable that the majority of the exhibited solution formation is occurring from the surface of the target materials, and that limited solution formation of the bulk material takes place. Indeed, consideration of the crystallite size of the materials indicates that the levels of solution formation occurring can be accounted for by considering the silver and vanadium located in the outermost layer of unit cells for the crystallites. If the observed solution formation is mostly a surface phenomenon, then the manner in which these materials terminate at the material/electrolyte interface would play a significant role in determining how much material is dissolved. Thus, while compositionally similar, differences in crystal structure of the materials could be significant. The possible edge configurations / crystal termination structures of the silver vanadium phosphorous oxide materials were considered and are discussed below.

Silver solution formation

The material $Ag_2VP_2O_8$ exhibited the highest level of silver solution formation. The structure of $Ag_2VP_2O_8$, looking down the b axis, is shown in Figure 2i. The lower boxed region of Figure 2i focuses on $Ag(2)^+$ ions located in a 6-sided tunnel comprised of corner sharing VO_6 and PO_4 polyhedra. Figure 2ii focuses on the $Ag(2)^+$ ion located at the edge of this 6-sided tunnel, where it can be located above the plane of VO_6 and PO_4 polyhedra at the edge of a crystal coordinated to five oxygen bonds ranging from 2.42 A - 3.05 Å. In this location the Ag^+ is not fully coordinated by vanadium oxide and phosphorous oxide polyhedra and thus may be more susceptible to solution formation into the electrolyte. The $Ag(1)^+$ ion may also be above the surface of $Ag_2VP_2O_8$, as it is also located in tunnels made from VO_6 and PO_4 polyhedra. The Ag^+ at the surface is not fully coordinated when above the VP_2O_8 host lattice (Figure 2iii) and thus may be more susceptible to solution formation or ion exchange by Li^+ ion from the electrolyte salt.

The two other SVPO materials, $Ag_{0.49}VOPO_4 \cdot 1.9H_2O$ and $Ag_2VO_2PO_4$, exhibited average normalized Ag solution formation levels lower than $Ag_2VP_2O_8$. Figure 1i shows the structure of $Ag_{0.49}VPO_4 \cdot 1.9H_2O$ viewed along the b axis,

emphasizing the layers of the V-O-P-O framework with Ag^+ ions and water molecules located between the layers. Figure 1ii shows the proposed coordination environment of Ag^+ ions at the edge of the structure. We propose that the layered structure terminates with Ag fully coordinated with six oxygen atoms: four oxygen atoms associated with H_2O molecules forming shorter bonds (2.4-2.57 A), and the two other oxygen atoms association with VPO layer framework forming longer bonds (2.65 A). As the Ag^+ ions are fully coordinated and not above the VPO layer framework, they would be less likely to dissolve via coordination with solvent and/or ion exchange with the lithium based electrolyte salt.
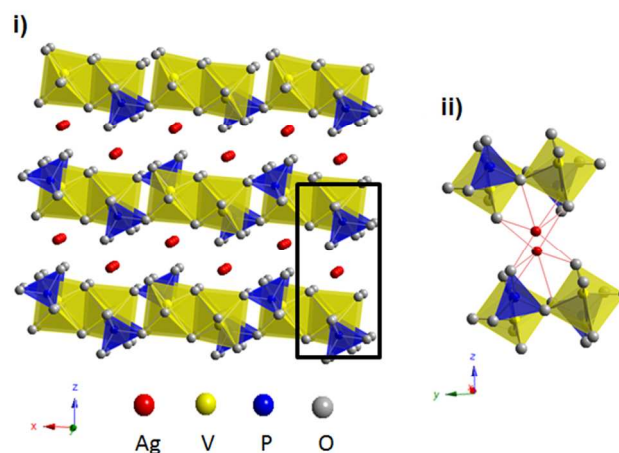

Figure 10i. Crystal structure of $Ag_2VO_2PO_4$ looking down the b axis. **ii.** Fully coordinated Ag^+ ions at the structure edge.

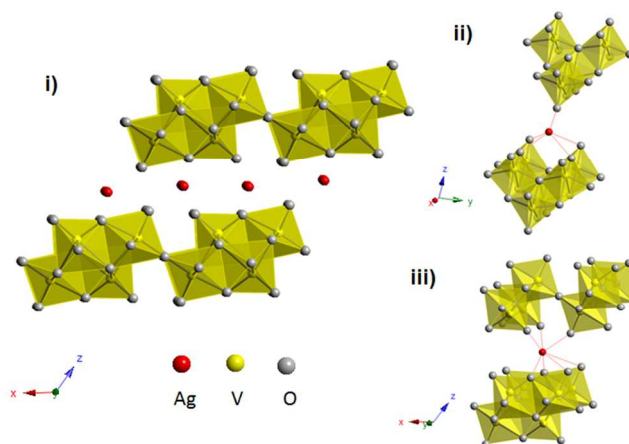**Figure 11i.** Crystal structure of $Ag_2V_4O_{11}$. Two possible coordination environments for Ag^+ ions at the terminating edge of the crystal are **ii.** the Ag^+ is partially coordinated by five oxygen atoms and **iii.** the Ag^+ is fully coordinated by 7 oxygen atoms.

The third layered structure, $Ag_2VO_2PO_4$, is shown in Figure 10i, with octahedral coordinated silver ions located between layers of edge sharing VO_6 octahedra and PO_4 tetrahedra. This material exhibited the lowest level of normalized Ag solution formation. For this layered structure, we propose that Ag^+ ions are fully coordinated by five oxygen atoms at the surface of the crystal, as illustrated in Figure 10ii. As with $Ag_{0.49}VOPO_4 \cdot 1.9H_2O$, these Ag^+ ions are less likely to be solvated or to undergo ion exchange because they are not

positioned above the VPO layer framework and instead are fully coordinated as in the bulk of the crystal lattice.

The fourth target material from which solution formation was studied is silver vanadium oxide, $Ag_2V_4O_{11}$. This material exhibited silver solution formation higher than that of $Ag_{0.49}VOPO_4·1.9H_2O$ and $Ag_2VO_2PO_4$ and lower than $Ag_2VP_2O_8$. Figure 11i illustrates the crystal structure of $Ag_2V_4O_{11}$ looking down the [010] direction. Its layers are comprised of edge and corner sharing distorted VO_6 octahedra. Silver ions are located between these layers where they are coordinated to seven oxygen atoms. For this material, there are two distinct possibilities for how the edge of the crystal structure terminates. The first possible structure is shown in Figure 11ii, where the Ag^+ ion at the crystal edge is coordinated by five oxygen atoms. In this configuration, Ag^+ ions are more likely to be solvated by the electrolyte. In the second structure, shown in Figure 11iii, the Ag^+ ion is fully coordinated by seven oxygen atoms, as occurs in the bulk of the crystal lattice, and will be less susceptible to solution formation. The $Ag_2V_4O_{11}$ material exhibits an intermediate level normalized Ag solution formation, attributed to the two Ag^+ ion termination structures described above.

Vanadium solution formation

As indicated in Figure 5, the materials $Ag_{0.49}VOPO_4·1.9H_2O$ and $Ag_2V_4O_{11}$ had levels of normalized vanadium solution formation which were approximately 3X that of the materials, $Ag_2VP_2O_8$ and $Ag_2VO_2PO_4$. All three phosphate based compounds have an interconnected lattice consisting of corner sharing vanadium oxide octahedra and phosphorous oxide tetrahedra. In contrast with the Ag^+ ions in these materials, vanadium ions are likely to be completely coordinated with oxygen atoms due to their high oxidation state. The level of distortion of vanadium oxide polyhedra in the various materials was considered in order to rationalize the solution formation data. For each material, the vanadium oxide octahedron is considerably distorted with one shorter bond (1.57-1.62 Å), one longer bond (2.15-2.41 Å) and four equatorial bonds ranging from 1.69 to 2.13 Å. In $Ag_2VP_2O_8$, five of the six oxygen atoms coordinated to vanadium oxide octahedra are also coordinated with phosphate tetrahedra including the longest bond 2.15 Å. In $Ag_2VO_2PO_4$, two of the six oxygen atoms coordinated to vanadium oxide are coordinated with phosphate tetrahedra. The longest V-O bond (2.31Å) and a bond of shorter length (1.68Å) share an edge with an adjacent vanadium oxide octahedron. In the oxide material $Ag_2V_4O_{11}$, the longest bonds share an edge with an adjacent vanadium oxide octahedron. However, the absence of phosphate tetrahedra with strong, short P-O bonds (1.53 Å on average for the three phosphate materials) may make the layer framework more susceptible to solvation by the electrolyte.

In previous work,[18, 21] we theorized that the phosphate based material $Ag_2VO_2PO_4$ was less prone to vanadium solution formation compared with $Ag_2V_4O_{11}$ due to the presence of stabilizing PO_4^{3-} polyanions in the lattice.[14] However, in this study, the phosphate based material $Ag_{0.49}VOPO_4·1.9H_2O$ exhibited normalized vanadium solution formation values higher than those of the other two silver vanadium phosphorous oxide materials. A detrimental effect of acidic contamination due to the presence of water in carbonate based electrolytes was previously noted for lithium iron phosphate based cathodes,

resulting in increased solubility of iron species.[17, 33] In order to elucidate the potential impact of the presence of water in the $Ag_{0.49}VOPO_4·1.9H_2O$, water content of the electrolytes exposed to the target materials were measured post experiment. The electrolyte samples exposed to $Ag_{0.49}VOPO_4·1.9H_2O$ had a water content of 160 ± 50 ppm, compared with water contents of 110 ± 30, 100 ± 30, and 100 ± 30 for $Ag_2VO_2PO_4$, $Ag_2VP_2O_8$, and $Ag_2V_4O_{11}$, respectively. Thus, it was unclear if the higher average water content of the electrolyte samples exposed to $Ag_{0.49}VOPO_4·1.9H_2O$ was a significant contributing factor regarding the higher vanadium solution formation for $Ag_{0.49}VOPO_4$ relative to $Ag_2VO_2PO_4$ and $Ag_2VP_2O_8$. To further probe this possibility, solution formation studies were conducted in both PC 1M $LiBF_4$ and PC 1M $LiBF_4$ + 600 ppm H_2O for all four materials. After 3 hours of stirring the $Ag_{0.49}VOPO_4·1.9H_2O$ in the electrolyte solutions, the concentrations of silver dissolved were 4.1 mg/L and 2.7 mg/L for the wet and dry electrolyte solutions, respectively, indicating that the added water enhanced the solution formation of silver. In contrast, the concentration of vanadium dissolved into the wet and dry electrolytes after three hours of stirring was 0.1 mg/L. Thus, it is unlikely that the water dissolving into the electrolyte from the $Ag_{0.49}VOPO_4·1.9H_2O$ material was the cause of the high vanadium concentration compared with the other two silver vanadium phosphorous oxide materials. Similar results were observed when water was added to the electrolyte solution formation medium for $Ag_2VO_2PO_4$, $Ag_2VP_2O_8$, and $Ag_2V_4O_{11}$. In each case, the wet electrolyte solution enhanced the solubility of silver, but had no noticeable effect on the solution formation of vanadium.

Although the addition of water to the electrolyte did not influence the solution formation of vanadium, because the structure of $Ag_{0.49}VOPO_4·1.9H_2O$ contains coordinated water molecules, the vanadium oxide/ phosphate layered framework may be more susceptible to solution formation. Four of the six oxygens which comprise the vanadium oxide octahedron are shared with PO_4^{3-} tetrahedra, however, the long (V-O) bond belongs to a water molecule, where incomplete coordination of vanadium upon loss of water from the lattice may make the vanadium more susceptible to solution formation. $Ag_{0.49}VOPO_4·1.9H_2O$ is also unique from the other materials in that the vanadium has a mixed oxidation state of ~4.5. It is expected that V^{5+} and V^{4+} are disordered within the VPO layers. This disorder may result in instability and thus susceptibility to solvation by the electrolyte.

Results from the differential scanning calorimetry experiments on the target materials support the hypothesis of weaker framework structure for $Ag_{0.49}VOPO_4·1.9H_2O$ relative to the other phosphorous oxide materials. $Ag_2VO_2PO_4$ has an endothermic transition at 540°C, while $Ag_2VP_2O_8$ has no transitions up to 580°C. In contrast, $Ag_{0.49}VPO_4·1.9H_2O$ shows numerous endothermic transitions, between 100 and 580°C, which indicates that less energy is needed to change the lattice structure of $Ag_{0.49}VPO_4·1.9H_2O$.

Conclusions

This study describes the appearance of silver and vanadium in solution from $Ag_{0.49}VOPO_4·1.9H_2O$ and $Ag_2VP_2O_8$, two members of the silver vanadium phosphorous oxide $(Ag_wV_xP_yO_z)$ family of materials. The vanadium concentration versus time data for both materials was consistent with the Noyes-Whitney model, which represents a diffusion controlled

solution formation process. In contrast, the silver concentration versus time data for both materials proceeded at a faster initial rate and was modelled using the Weibull function, indicative of a more complex mechanism than simple solution formation. Significantly lower levels of silver were observed when testing was done without electrolyte salt, providing evidence that the presence of Li^+ ions in the electrolyte plays a large role in the silver in solution mechanism.

The solution data of $Ag_{0.49}VOPO_4 \cdot 1.9H_2O$ and $Ag_2VP_2O_8$ was compared with $Ag_2VO_2PO_4$ and $Ag_2V_4O_{11}$, two additional materials for which solution formation has recently been described, in order to probe the influence of stoichiometry and crystal structure on solution formation. The trace levels of cathode in solution suggest that the solution formation processes are strongly influenced by the crystal structure at the surface of the material crystallites. As such, possible crystal termination / edge configuration structures of the target materials were considered with regards to the solution formation results. Higher levels of normalized silver solution formation occurred in those materials in which incomplete silver coordination environments at the crystal edge were possible. For vanadium, increased solution formation was observed for the oxide material $Ag_2V_4O_{11}$ as well as for the phosphate oxide $Ag_{0.49}VOPO_4 \cdot 1.9H_2O$. Increased susceptibility to vanadium solution formation for $Ag_{0.49}VOPO_4 \cdot 1.9H_2O$ may be associated with structural water or the existence of multiple vanadium oxidation states.

This systematic investigation of multiple materials identifies the most promising members of the SVPO family for reducing vanadium solution formation as $Ag_2VO_2PO_4$ and $Ag_2VP_2O_8$. The low solution rates coupled with their electrochemical performance make these materials interesting alternatives to $Ag_2V_4O_{11}$ for the ICD application. More broadly, the results presented here provide a framework for the quantitative and kinetic analyses of the dissolution of cathode materials which will aid the broader community in more fully understanding this battery failure mechanism.

Acknowledgements

Notes and references

a Department of Chemistry, Stony Brook University, Stony Brook, NY 11794.

b Department of Materials Science and Engineering, Stony Brook University, Stony Brook, NY 11794.

c Brookhaven National Laboratory, Upton, NY 11973.

* corresponding authors: (KJT) kenneth.takeuchi.1@stonybrook.edu, (ACM)   amy.marschilok@stonybrook.edu,   (EST) esther.takeuchi@stonybrook.edu

† Footnotes should appear here. These might include comments relevant to but not central to the matter under discussion, limited experimental and spectral data, and crystal data.

1. D. C. Bock, A. C. Marschilok, K. J. Takeuchi and E. S. Takeuchi, *Electrochim. Acta*, 2012, 84, 155-164.
2. G. G. Amatucci, J. M. Tarascon and L. C. Klein, *Solid State Ionics*, 1996, 83, 167-173.
3. A. du Pasquier, A. Blyr, P. Courjal, D. Larcher, G. Amatucci, B. Gerand and J. M. Tarascon, *Journal of the Electrochemical Society*, 1999, 146, 428-436.
4. D. H. Jang and S. M. Oh, *Journal of the Electrochemical Society*, 1997, 144, 3342-3348.
5. T. Aoshima, K. Okahara, C. Kiyohara and K. Shizuka, *Journal of Power Sources*, 2001, 97-98, 377-380.
6. C.-H. Lu and S.-W. Lin, *J. Mater. Res.*, 2002, 17, 1476-1481.
7. S. Jouanneau, G. L. S. A. Le, A. Verbaere and D. Guyomard, *Journal of the Electrochemical Society*, 2005, 152, A1660-A1667.
8. K. J. Takeuchi, A. C. Marschilok, S. M. Davis, R. A. Leising and E. S. Takeuchi, *Coordination Chemistry Reviews*, 2001, 219-221, 283-310.
9. E. S. Takeuchi and P. Piliero, *Journal of Power Sources*, 1987, 21, 133-141.
10. R. A. Leising and E. S. Takeuchi, *Chemistry of Materials*, 1993, 5, 738-742.
11. R. A. Leising and E. S. Takeuchi, *Chemistry of Materials*, 1994, 6, 489-495.
12. E. S. Takeuchi, *Journal of Power Sources*, 1995, 54, 115-119.
13. M. J. Root, *Journal of the Electrochemical Society*, 2011, 158, A1347-A1353.
14. B. L. Ellis, K. T. Lee and L. F. Nazar, *Chemistry of Materials*, 2010, 22, 691-714.
15. D.-H. Kim and J. Kim, *Electrochemical and Solid-State Letters*, 2006, 9, A439-A442.
16. N. Iltchev, Y. Chen, S. Okada and J.-i. Yamaki, *Journal of Power Sources*, 2003, 119-121, 749-754.
17. M. Koltypin, D. Aurbach, L. Nazar and B. Ellis, *Electrochemical and Solid-State Letters*, 2007, 10, A40-A44.
18. D. C. Bock, A. C. Marschilok, K. J. Takeuchi and E. S. Takeuchi, *Journal of Power Sources*, 2013, 231, 219-235.
19. D. C. Bock, K. J. Takeuchi, A. C. Marschilok and E. S. Takeuchi, *Dalton Transactions*, 2013, 42, 13981-13989.
20. A. C. Marschilok, Y. J. Kim, K. J. Takeuchi and E. S. Takeuchi, *Journal of the Electrochemical Society*, 2012, 159, A1690-A1695.
21. Y. J. Kim, C.-Y. Lee, A. C. Marschilok, K. J. Takeuchi and E. S. Takeuchi, *Journal of Power Sources*, 2011, 196, 3325-3330.
22. E. S. Takeuchi, C.-Y. Lee, P.-J. Cheng, M. C. Menard, A. C. Marschilok and K. J. Takeuchi, *Journal of Solid State Chemistry*, 2013, 200, 232-240.
23. J. Vetter, P. Novak, M. R. Wagner, C. Veit, K. C. Moeller, J. O. Besenhard, M. Winter, M. Wohlfahrt-Mehrens, C. Vogler and A. Hammouche, *Journal of Power Sources*, 2005, 147, 269-281.
24. D. H. Jang, Y. J. Shin and S. M. Oh, *Journal of the Electrochemical Society*, 1996, 143, 2204-2211.
25. A. Blyr, C. Sigala, G. Amatucci, D. Guyomard, G. Y. Chabre and J. M. Tarascon, *Journal of the Electrochemical Society*, 1998, 145, 194-209.
26. C. Zhan, J. Lu, A. J. Kropf, T. Wu, A. N. Jansen, Y.-K. Sun, X. Qiu and K. Amine, *Nature Communications*, 2013, 4, 3437, 3438 pp.
27. M. Ochida, Y. Domi, T. Doi, S. Tsubouchi, H. Nakagawa, T. Yamanaka, T. Abe and Z. Ogumi, *Journal of the Electrochemical Society*, 2012, 159, A961-A966.
28. C. Delacourt, A. Kwong, X. Liu, R. Qiao, W. L. Yang, P. Lu, S. J. Harris and V. Srinivasan, *Journal of the Electrochemical Society*, 2013, 160, A1099-A1107.
29. S. Jouanneau, A. Verbaere, S. Lascaud and D. Guyomard, *Solid State Ionics*, 2006, 177, 311-315.
30. X.-W. Gao, J.-Z. Wang, S.-L. Chou and H.-K. Liu, *Journal of Power Sources*, 2012, 220, 47-53.

31. Q. Shi, R. Hu, M. Zeng, M. Dai and M. Zhu, *Electrochim. Acta*, 2011, 56, 9329-9336.
32. D. Aurbach, B. Markovsky, A. Rodkin, E. Levi, Y. S. Cohen, H. J. Kim and M. Schmidt, *Electrochim. Acta*, 2002, 47, 4291-4306.
33. E. Markevich, G. Salitra and D. Aurbach, *Electrochemistry Communications*, 2005, 7, 1298-1304.
34. D. Aurbach, B. Markovsky, G. Salitra, E. Markevich, Y. Talyossef, M. Koltypin, L. Nazar, B. Ellis and D. Kovacheva, *Journal of Power Sources*, 2007, 165, 491-499.
35. H. Y. Kang, S. L. Wang, P. P. Tsai and K. H. Lii, *Journal of the Chemical Society, Dalton Transactions: Inorganic Chemistry (1972-1999)*, 1993, 1525-1528.
36. P. Ayyappan, A. Ramanan and C. C. Torardi, *Inorganic Chemistry*, 1998, 37, 3628-3634.
37. A. Daidouh, M. L. Veiga and C. Pico, *Journal of Solid State Chemistry*, 1997, 130, 28-34.
38. A. A. Noyes and W. R. Whitney, *Journal of the American Chemical Society*, 1897, 19, 930-934.
39. A. Dokoumetzidis and P. Macheras, *International Journal of Pharmaceutics*, 2006, 321, 1-11.
40. W. Weibull, *Journal of Applied Mechanics*, 1951, 18, 293-297.
41. F. Langenbucher, *Journal of Pharmacy and Pharmacology*, 1972, 24, 979-981.
42. P. Macheras and A. Dokoumetzidis, *Pharmaceutical Research*, 2000, 17, 108-112.
43. P. Costa and J. M. Sousa Lobo, *European Journal of Pharmaceutical Sciences*, 2001, 13, 123-133.
44. S. D'Souza Susan, A. Faraj Jabar and P. DeLuca Patrick, *AAPS PharmSciTech*, 2005, 6, E553-564.
45. L. Van Vooren, G. Krikilion, J. Rosier and B. De Spiegeleer, *Drug Development and Industrial Pharmacy*, 2001, 27, 885-892.
46. C.-W. Lin and T.-M. Cham, *Int. J. Pharm.*, 1996, 127, 261-272.
47. P. M. Sathe and J. Venitz, *Drug Development and Industrial Pharmacy*, 2003, 29, 349-355.
48. E. Chevalier, M. Viana, A. Artaud, L. Chomette, S. Haddouchi, G. Devidts and D. Chulia, *AAPS PharmSciTech*, 2009, 10, 597-605.
49. R. C. Nagarwal, D. N. Ridhurkar and J. K. Pandit, *AAPS PharmSciTech*, 2010, 11, 294-303.
50. M. V. S. Varma, A. M. Kaushal and S. Garg, *Journal of Controlled Release*, 2005, 103, 499-510.
51. L. S. Koester, G. G. Ortega, P. Mayorga and V. L. Bassani, *European Journal of Pharmaceutics and Biopharmaceutics*, 2004, 58, 177-179.
52. E. Adams, D. Coomans, J. Smeyers-Verbeke and D. L. Massart, *Int. J. Pharm.*, 2002, 240, 37-53.
53. M. C. Bonferoni, S. Rossi, F. Ferrari, M. Bertoni, G. K. Bolhuis and C. Caramella, *Journal of Controlled Release*, 1998, 51, 231-239.
54. V. Papadopoulou, K. Kosmidis, M. Vlachou and P. Macheras, *Int J Pharm*, 2006, 309, 44-50.